Removal of COD, NH_4-N, and perfluorinated compounds from wastewater treatment plant effluent using ZnO-coated activated carbon

Jiawei Tang, Yu Liu, Peidong Su, Jingwei Quan, Yufeng Hu, Wenqian Wang and Chunhui Zhang

ABSTRACT

This study investigated the removal of chemical oxygen demand (COD), NH_4-N, and perfluorinated compounds (PFCs) in the effluent from a wastewater treatment plant (WWTP) using ZnO coated activated carbon (ZnO/AC). Results suggested that the optimal dosage of the ZnO/AC was 0.8 g/L within 240 min of contact time, at which the maximum removal efficiency of COD was approximately 86.8%, while the removal efficiencies of PFOA and PFOS reached 86.5% and 82.1%. In comparison, the removal efficiencies of NH_4-N, PFBA, and PFBS were lower, at approximately 47.9%, 44.0%, and 55.4%, respectively. In addition, COD was preferentially adsorbed before PFCs and NH_4-N, when the contact time ranged from 0 to 180 min, and the order of PFCs removal showed a positive correlation with C-F chain length. The kinetic study revealed that the removal of COD, NH_4-N, and PFCs could be better depicted and predicted by the Lagergren quasi-second order dynamic model with high correlation coefficients, which involved liquid membrane diffusion, intraparticle diffusion, and photocatalytic reactions. The saturated ZnO/AC was finally regenerated using ultrasound for 3 h and retained excellent performance, which proved it could be considered as an effective and alternative technology.

Key words | activated carbon, COD, NH_4-N, PFCs, ZnO

Jiawei Tang
Yu Liu
Yufeng Hu
Wenqian Wang
Chunhui Zhang (corresponding author)
School of Chemical & Environmental Engineering,
China University of Mining & Technology (Beijing),
Beijing 100083,
China
E-mail: *zchcumtb@hotmail.com*

Peidong Su
College of Chemistry and Environmental Engineering,
Shenzhen University,
Shenzhen 518060,
China
and
Key Laboratory of Drinking Water Science and Technology, Research Center for Eco-Environmental Sciences,
Chinese Academy of Sciences,
Beijing 100085,
China

Jingwei Quan
School of Civil and Environmental Engineering,
University of New South Wales,
Sydney 2033,
Australia

HIGHLIGHTS

- The ZnO-coated activated carbon was prepared via a homogeneous precipitation method.
- Enhanced removal of PFCs in effluent using ZnO/AC absorbent was developed.
- The optimum parameters, kinetics, and mechanism of PFCs removal were investigated.

INTRODUCTION

Perfluorinated compounds (PFCs) are a class of fluorine-containing chemicals that have been used worldwide in plastic, rubber, leather, and other consumer and industrial products (Tomy *et al.* 2009; Fromme *et al.* 2010; Ansari *et al.* 2016). Due to the high C-F bond energy (116 kcal/mol), PFCs show thermal stability and repel both water and oil, making them generally resistant to degradation and thus persistent in the environment (Jian *et al.* 2017; Wang *et al.* 2018). The long-chain analogues (C-F chain length $\geq$7), such as perfluorooctanoic acid (PFOA) and perfluorooctane sulfonate (PFOS) with hydrophilic/oleophobic properties, are the anionic surfactants most frequently detected in the environment (Sorlini *et al.* 2015; Fagbayigbo *et al.* 2018). Owing to their persistency, bioaccumulation and toxicity, PFCs have become a hotspot in recent studies. A study of the occurrence of PFCs in New Jersey public drinking water systems found that PFOA was the most commonly detected PFC (57% of samples) with a maximum

doi: 10.2166/wst.2020.308

concentration of 100 ng/L. Both PFOS and PFOA were also found in infant blood at average concentrations of 4.2 ng/mL and 2.67 ng/mL, respectively (Niu *et al.* 2013).

Chronic exposure to PFCs may cause hepatotoxicity, neurotoxicity, behavioral disability, and genetic defects that exhibit toxicity to human health (Seo *et al.* 2018). Various advanced treatment methods include, but are not limited to, adsorption, ultrasound-chemical treatment, membrane filtration, and electrochemical technologies (Moriwaki *et al.* 2005; Yu *et al.* 2014). These treatments have been extensively reported to degrade PFCs in prepared solutions (Hori *et al.* 2006; Niu *et al.* 2017). Considering factors such as processing costs, operating conditions, and convenient operation, adsorption is a promising method for the removal of PFCs from an aqueous solution (Ochoa-Herrera & Sierra-Alvarez 2008; Aydin *et al.* 2008; Senevirathna *et al.* 2010). Adsorbents such as activated carbon, zeolite, and silica gels used for the removal of PFCs from wastewater were well studied (Zhang *et al.* 2018; Su *et al.* 2019). Heterogeneous photocatalytic materials were also introduced as adsorbents because of their high efficiency in organic pollutant degradation in wastewater (Raizada *et al.* 2014). ZnO has been widely employed in the treatment of organic pollutants due to its optical and electronic properties (band gap = 3.37 eV), chemical stability, and non-toxicity among various semiconductor photocatalysts (Yong *et al.* 2016).

Most recent studies were performed on laboratory-prepared solutions, while limited data exist for the removal of PFCs in wastewater treatment plant (WWTP) effluent. Considering that a practical wastewater sample contains a variety of contaminants with mutual interference amongst them, the use of a laboratory-prepared water sample does not accurately simulate it. In this study, ZnO-coated activated carbon (ZnO/AC) was synthesized using a homogeneous precipitation method, and employed to remove PFCs in the effluent from a WWTP. The comparative removal performance of PFCs and other contaminants (i.e., chemical oxygen demand (COD) and NH_4-N) from the effluent using ZnO/AC adsorbent was investigated.

MATERIALS AND METHODS

Materials

The chemicals include methanol (GR), methyl tert butyl ether (MTBE, 99%), ammonium acetate (chromatographic purity), zinc nitrate ($Zn(NO_3)_2{\cdot}6H_2O$, AR), carbamide (CON_2H_4, AR), ethanol (CH_3OH, AR), glacial acetic acid (GR, >99.8%) and ammonia (GR, 50% v/v). Perfluorobutanoic acid (PFBA), PFOA, perfluorobutane sulfonate (PFBS), PFOS, perfluorodecanoic acid (PFDA), perfluorohexanoic acid (PFHxA), perfluoroheptanoic acid (PFHpA), perfluorononanoic acid (PFNA) and perfluorohexyl sulfonic acid (PFHxS) were obtained from Sigma-Aldrich company (USA). Quantitative mixed standard includes quantitative mixed standard PFAC-MXB, internal standard $^{13}C_4$-PFOS, internal standard $^{13}C_4$-PFOA, and internal standard $^{13}C_4$-PFBA, which were purchased from Wellington Laboratories (Canada). Deionized (DI) water was prepared by the Milli-Q Advantage A 10 system (Millipore, USA) at a resistivity of 18.2 M·Ω. The filter membrane (0.45 μm, glass fiber filter) was purchased from Sartorius Stedim Biotech company. The Oasis WAX 6 cc pre-processing column was purchased from Waters company (USA).

Water sample collection

The practical wastewater used in this study was collected from the effluent of a WWTP in Miyun District, Beijing, which is near a food processing factory and an automobile repair workshop. This plant has a treatment capacity of 800 m^3/d by employing a typical Anaerobic-Anoxic-Oxic (A^2/O) system. The detailed operational conditions of this WWTP are: mixed liquor suspended solids (MLSS) concentration = 1,600 ± 150 g/m^3, solids retention time (SRT) = 6 d and hydraulic retention time (HRT) = 5.0 h). All the wastewater samples were stored in polymeric plastic bottles at 4 °C before use. The pH of the water sample was measured to be 6.8 ± 0.2 on site with a pH meter (Orion GS9156, Thermo Fisher Scientific Inc.). The concentrations of COD, BOD_5, NH_4-N, TP were 92 ± 2.8, 28.5 ± 3.3, 11.2 ± 1.5, and 0.9 ± 0.2 mg/L, respectively, after being filtered with a microfiltration membrane (0.45 μm, glass fiber filter) according to the standard methods of China (Xi *et al.* 2008).

Synthesis and characterization of ZnO/AC

ZnO/AC adsorbent was prepared by the homogeneous precipitation method using $Zn(NO_3)_2{\cdot}6H_2O$ and CON_2H_4 according to the previous report, with minor modification (Raizada *et al.* 2014). In a typical procedure, the commercial coal-based activated carbon was first washed with DI water until there was no obvious change in pH, then dried in an oven at 105 °C. $CO(NH_2)_2$ and $Zn(NO_3)_2{\cdot}6H_2O$ were accurately weighed to a molar ratio of 1:5, which was previously

determined to dissolve in 50 mL of DI water. After homogeneous mixing, the solution was diluted to 200 mL. Then, 10 g of activated carbon was added and the slurry was placed into a pressure steam sterilizing pot (0.2 MPa) to react for a period of 2 h under 121 °C to obtain the ZnO/AC precursor. The ZnO/AC precursor was then calcined in a tubular furnace (N_2 protection) at 500 °C for 2 h to harvest the final product.

The textural characteristics of the ZnO/AC were recorded by N_2 gas adsorption isotherms at −196 °C using an ASAP 2020 (Micromeritics). Before adsorption experiments, the ZnO/AC sample was degassed at 150 °C under a vacuum of 10^{-6} Torr (Micromeritics). The iodine value (IV) and methylene blue value (MBV) were used to characterize the pore structure of these absorbent samples by the standard method (Iodine number, China method GB/T 7702.7-2008, and methylene blue adsorption, China method GB/T 7702.6-2008). The morphologies and elemental composition of the ZnO/AC sample were examined by a Nova nano scanning electron microscope (SEM) (s4800, Hitachi Co. Ltd) and energy dispersive spectrum (EDS) (EX250, Horiba Co. Ltd, Japan).

Batch adsorption experiment

To evaluate the adsorption capacity of synthesized ZnO/AC absorbent, batch adsorptive experiments of wastewater were conducted at various conditions. For a single adsorption, a total amount of 0.2–1.2 g of absorbents was added into 1.0 L of filtered effluent sample, and then 100 mL of prepared sample solution was poured into a 250 mL conical flask respectively before they were rotated on a horizontal vibration water bath while processing. The effects of adsorbent dosage (0.2–1.2 g/L) and contact time (0–5 h) on the adsorption performance were investigated according to the removal efficiencies of PFCs. Besides, to verify the ZnO photocatalytic effect on the removal of contaminants in the wastewater, multi-group parallel experiments were carried out under solar irradiation (Site: Haidian District, Beijing, outdoors, average temperature: 34 ± 3 °C, Grade of UV Index: 4, UV radiation: 15–30 W/m^2, experiment duration: 11 a.m. to 15 p.m.) and dark environment (Laboratory room, temperature: 26 ± 2 °C), respectively. Subsequently, the saturated ZnO/AC absorbent was regenerated by ultrasonic process for different times (1–4 h).

Data analysis

PFCs were analyzed by using high performance liquid chromatography (HPLC) with a dual pump and autosampler (Ultimate 3000, ThermoFisher Scientific), coupled to electrospray ionization tandem mass spectrometry, and a Chromeleon 6.70 chromatography workstation (American Dionex Company). The analysis column was an Acclaim 120 C18 column (4.6 × 150 mm, 5 μm, American Dionex Company). The sample volume was set to 10 μL with 1 μL/min of flow rate. The two internal standards (2 ng $^{13}C_4$-PFOA and 2 ng $^{13}C_4$-PFOS) were mixed with other standard solution and added to the samples before extraction. The recovery and reproducibility of PFCs in filtered samples ranged from 79% to 113%, and the coefficients of determination (r^2) of calibration curves for target analytes were all higher than 0.995. The limit of detection (LOD) was defined as the concentration that yielded a signal-to-noise (S/N) ratio of 3.0, while the limit of quantification (LOQ) was defined as the concentration that yielded a S/N ratio of 10. More details were described by our previous study (Shi *et al.* 2010). By using the above method, the PFCs of the filtered effluent sample was analyzed and the results are summarized in Table 1. As indicated, eight PFCs were

Table 1 | Concentration of PFCs in the effluent sample

PFCs	Abbreviation	Concentration (ng/L)	Molecular formula	C-F number	LOD (ng/L)	LOQ (ng/L)
Perfluorobutanoic acid	PFBA	76	$C_4HF_7O_2$	3	0.98	3.5
Perfluorobutane sulfonate	PFBS	88	$C_4F_9O_3S$	4	2.4	5.0
Perfluorohexanoic acid	PFHxA	55	$C_6HF_{11}O_2$	5	1.8	5.0
Perfluoroheptanoic acid	PFHpA	21	$C_7HF_{13}O_2$	7	1.36	5.0
Perfluorooctanoic acid	PFOA	166	$CF_3(CF_2)_6COOH$	7	0.62	2.1
Perfluorooctane sulfonate	PFOS	175	$C_8F_{17}KO_3S$	8	0.19	0.9
Perfluorononanoic acid	PFNA	43	$CF_3(CF_2)_7COOH$	8	0.98	3.2
Perfluorodecanoic acid	PFDA	34	$CF_3(CF_2)_8CO_2H$	9	2.07	6.9

detected in the wastewater and the concentration of PFOS was approximately 175 ng/L, followed by PFOA (166 ng/L), PFBS (88 ng/L) and PFBA (76 ng/L).

In the experimental process, the removal efficiency of PFCs (R_P) was calculated by Equation (1):

$$R_p = \frac{C_0 - C_t}{C_0} \times 100\% \quad (1)$$

where C_0 and C_t were the initial concentration of PFCs and the concentration of PFCs at time 't', respectively.

RESULTS AND DISCUSSION

Zno/AC characterization

Physical properties and adsorption characteristics of ZnO/AC

The physical properties of the original AC and ZnO/AC are summarized in Table 2. The granularity and filling proportion changed slightly after coating with ZnO. The IV increased from 820 mg/g to 995 mg/g and the MBV decreased from 155 mg/g to 130 mg/g, suggesting that the number of micropores of activated carbon increases, which is beneficial to the adsorption of micro-pollutants in water (Zhang *et al.* 2018). The pore width distribution and N_2 adsorption-desorption isotherms of ZnO/AC are presented in Figure 1. As shown in Figure 1(a), there was a strong peak in the range of 0.6–1.5 nm, followed by two weak peaks in the range of 3.0–6.0 nm and 6.0–12.0 nm respectively, which indicated that the ZnO/AC was mainly dominated by micropores. The N_2 adsorption-desorption isotherms of ZnO/AC (Figure 1(b)) exhibited a curve of type I according to the IUPAC classification, which further proved the ZnO/AC belonged to a microporous adsorbent. Additionally, when the value of P/P_0 was less than 1.0, the rapid rise of the N_2 adsorption isotherm implies that the pore diameters of ZnO/AC micropores and mesopores are close to the molecular diameters of adsorbate. When the value of P/P_0 ranged from 1.0 to 3.0, the N_2 adsorption isotherm tended to be gentle, indicating that non-microporous multi-layer adsorption occurs.

Table 2 | Characteristics of original AC and ZnO/AC absorbents

Parameter	Unit	Value	
		Original AC	ZnO/AC
Granularity	Mesh	15–20	10–20
Filling proportion	g/cm^3	0.47–0.52	0.46–0.55
Iodine adsorption value	mg/g	820	995
Methylene blue number	mg/g	155	130

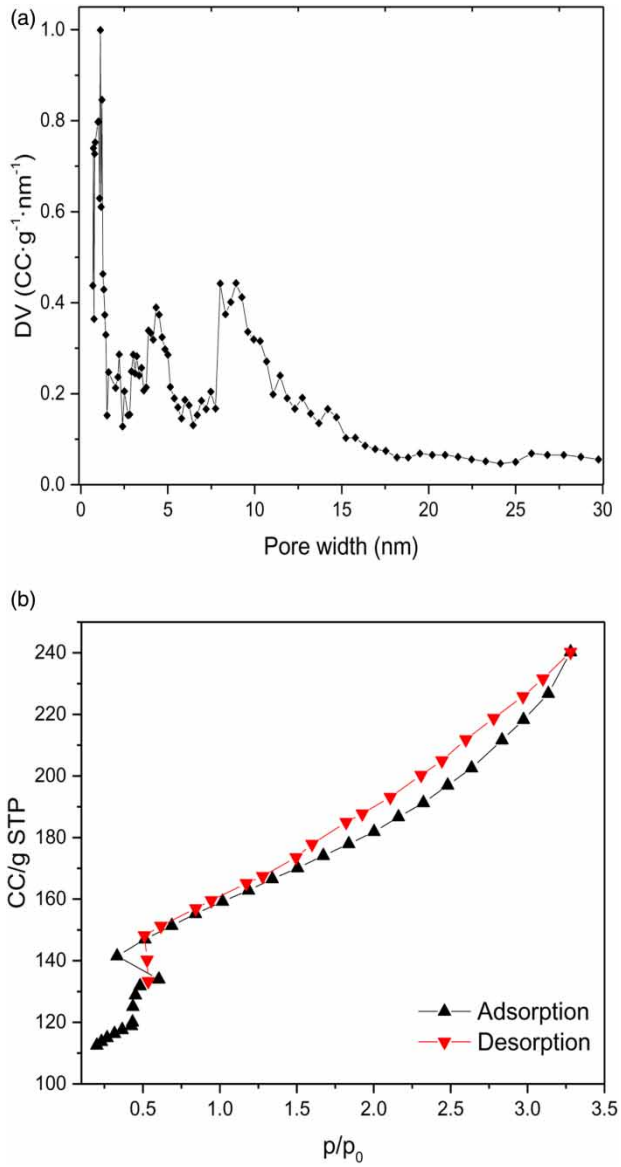

Figure 1 | Cumulative pore volume versus pore radius plots (a) and N_2 adsorption-desorption isotherms of ZnO/AC (b).

SEM–EDS analysis

The SEM images of the original AC and ZnO/AC are shown in Figure 2. The original AC (Figure 2(a)) exhibited an

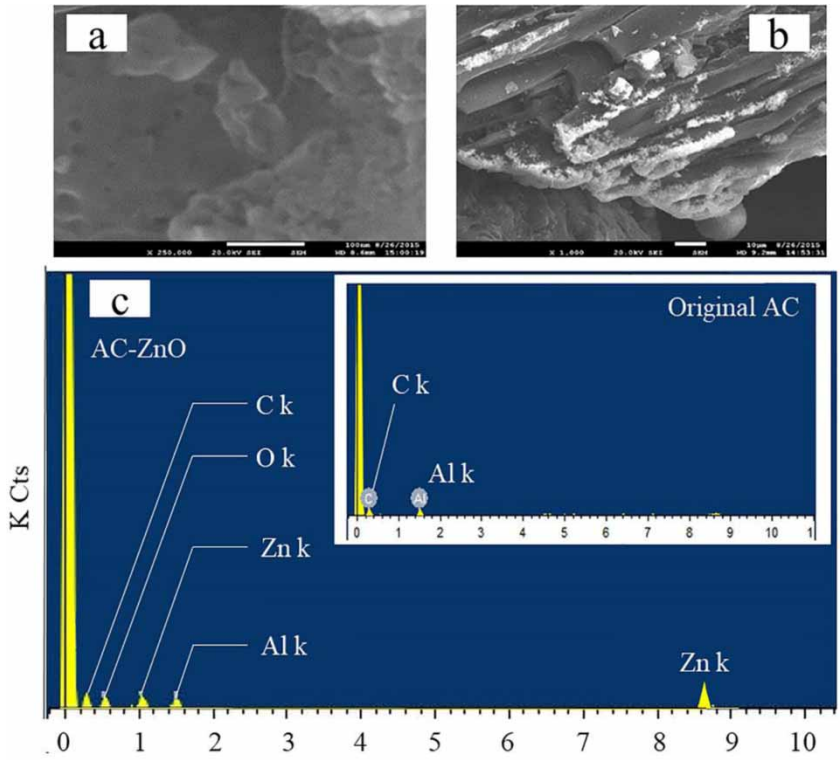

Figure 2 | SEM images of original AC (a) and ZnO/AC (b), and EDS energy spectrum of AC and ZnO/AC (c).

uneven porous surface, which provided the possibility for ZnO particles to be attached on the pores of AC. After being doped with ZnO and calcined at 500 °C, a white layer emerged on the surface of the ZnO/AC precursor (Figure 2(b)). The element distribution of the original AC and ZnO/AC are presented in Table 2 and Figure 2(c), from which it can be seen that the original AC contained approximately 88.61% (mass ratio) of C with 11.39% of Al. In comparison, 31.73% and 14.17% O and Zn were detected in the ZnO/AC, respectively.

Adsorption experiment

Effect of absorbent dosage

The effect of dosage on the removal performance with different amounts of adsorbents after 3 h of reaction time was carried out. To determine the photocatalytic effect of ZnO, batch adsorption experiments with ZnO/AC were performed in indoor (dark) and sunlight conditions (solar), respectively. In Figure 3(a), the COD removal efficiency increased significantly when the dosage of AC increased from 0.2 to 1.2 g/L. The COD removal efficiency could reach 74.6% when the dosage of AC ranged from 1.0 g/L to 1.2 g/L, which was close to the maximum removal efficiency (76.8%) of ZnO/AC in a dark environment. By comparison, the removal efficiency of COD was up to 86.8% with light irrigation. In this case, the order of removal efficiency of COD was ZnO/AC (solar) > ZnO/AC (dark) ≈ AC. Moreover, almost the same phenomenon was observed for other contaminants. With the dosage of the ZnO/AC (solar) ranging from 0.6 to 1.2 g/L, the maximum removal efficiencies of NH_4-N, PFOA, PFOS, PFBA and PFBS were 43.2 to 47.9%, 77.5 to 86.6%, 67.2 to 82.1%, 38.8 to 44% and 39.5 to 55.4% with solar light, respectively (Figure 3(b)–3(f)). According to the report from Lu & Zhou (2012), the radiation intensity of sunlight ranges from 700 to 1 000 W/m^2 from 12 p.m. to 14 p.m. on a sunny summer day (Jul. to Aug.), and the intensity of UV in Haidian District of Beijing was 15–30 W/m^2 (grade of UV index: 4) during the experimental process. Thus, it can be speculated that the partial ultraviolet light in sunlight promoted the photocatalytic reaction of ZnO particles to further degrade pollutants (Shibin *et al.* 2015). Besides, as the removal efficiencies of COD and PFCs did not increase further with the increase in the amount of absorbent (>0.8 g/L) added, the optimal absorbent dosage was determined to be 0.8 g/L for the following optimization experiment.

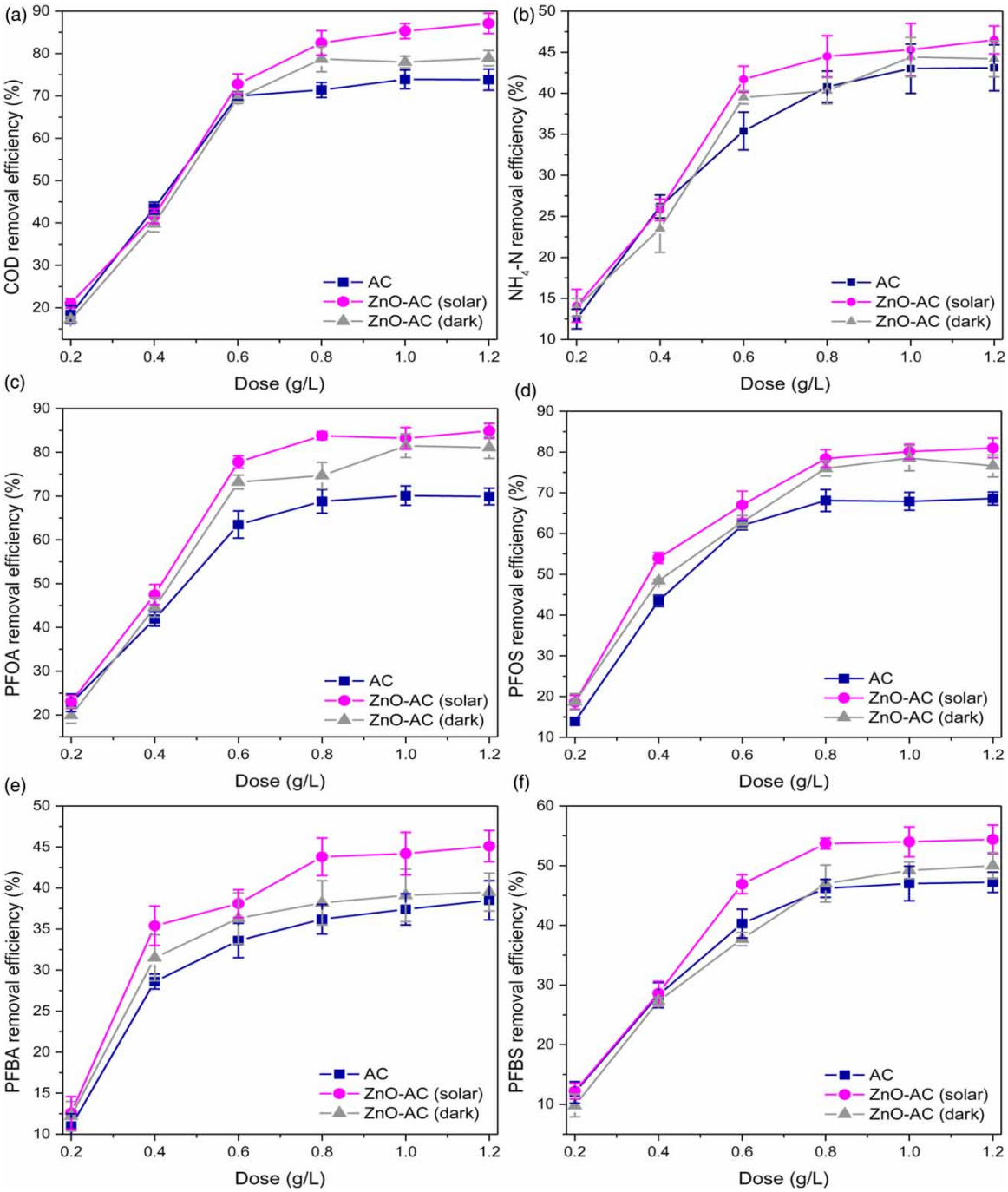

Figure 3 | Effect of absorbent dose on removal of COD (a), NH_4-N (b), PFOA (c), PFOS (d), PFBA (e), and PFBS (f).

Effect of contact duration

To evaluate the effect of contact duration on the removal of COD, NH_4-N and PFCs, the adsorption test was conducted with agitation in a laboratory (dark) and outdoor environment (solar), respectively for a period of 300 min. As depicted in Figure 4(a), the removal efficiency of COD increased rapidly to approximately 60% in 0–80 minutes, and reached the maximum value of 70.5% after 180 minutes by using AC absorbent, while the COD removal efficiency was 76.8% and 85.2% using ZnO/AC in the absence and presence of solar light, respectively. On the other hand,

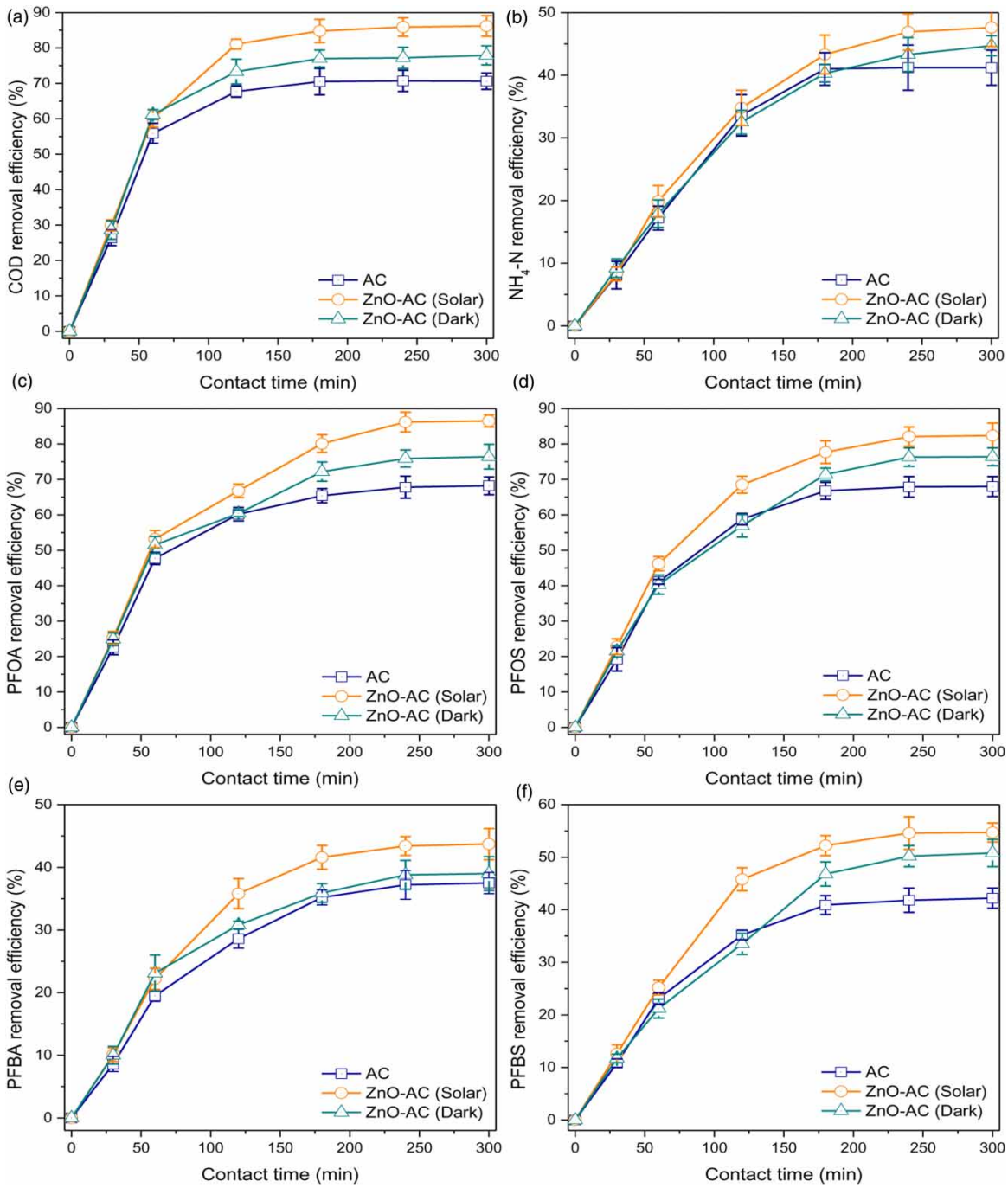

Figure 4 | Effect of contact duration on COD (a), NH_4-N (b), PFOA (c), PFOS (d), PFBA (e), and PFBS (f) removal.

these absorbents had a poor removal capacity for NH_4-N as their removal efficiencies only reached 41.2, 43.8 and 47.9% using AC, ZnO/AC (dark) and ZnO/AC (solar) after 240 min of contact time (Figure 4(b)). Figure 4(c)–4(f) present the removal performance of PFOA, PFOS, PFBA and PFBS. Obviously, the removal efficiencies of PFOA (68.2–86.5%) and PFOS (67.0–82.1%) were higher than that of PFBS (41.0–55.4%) and PFBA (37.5–44.0%) in all experiments, indicating the adsorption capacity of PFCs was AC < ZnO/AC (dark) < ZnO/AC (solar) as well. For the difference of COD and PFCs removal efficiencies by adsorbent in sunlight (solar) and indoor (dark)

environments, analysis of variance (ANOVA) was employed to reveal the contribution of sunlight to the effect of adsorbent application. As expected, it was demonstrated that the ZnO catalytic material had a significant contribution to the removal of COD and PFCs under sunlight, for their p-values were calculated as 0.0096 and 0.032, respectively. Notably, the removal efficiencies of PFBA (44.0%) and PFBS (55.4%) were much lower than that of PFOA and PFOS after 240 min of contact durations, which could be attributed to their strong hydrophilic group, and a shorter carbon chain made them less susceptible to degradation (Niu *et al.* 2013). Based on the above results, the optimal contact time was determined to be 240 min with the absorbent dosage of 0.8 g/L.

Competitive adsorption and kinetics

Since the organic matter, inorganic compounds, and NH_4-N existing in the wastewater might disturb the adsorption efficiency of PFCs, herein the competitive adsorption process was studied on the ZnO/AC (solar) at different contact durations. Furthermore, to further examine the competition of different kinds of perfluorocarbons, six perfluorocarbons (i.e. PFOA, PFOS, PFHxA, PFNA, PFBA, and PFBS) with different C-F chain lengths were also analyzed. As displayed in Figure 5(b), the removal efficiencies of PFOA and PFOS were higher than those PFCs with short C-F chains, which could be ascribed to the difference in the distribution coefficient value (K_d) of the PFCS (Arvaniti *et al.* 2012). Despite the higher initial concentration of PFOA and PFOS possessed, the carbon-rich substances of PFCs were more preferentially adsorbed on the adsorbents than the short C-F chain ones under the competitive adsorption process, which was consistent with the previous result (Maneerung *et al.* 2016).

As the adsorption competition could be caused by the co-existence of pollutants such as the organic matter, inorganic compounds and NH_4-N, it is significant for investigating the adsorption kinetics to reveal the mechanism of the adsorption process. Therefore, to further investigate the adsorption behavior of COD, NH_4-N and PFCs by ZnO/AC (light), the Lagergren quasi-first (Equation (2)) and Lagergren quasi-second order dynamic equation (Equation (3)) were employed (Zhou *et al.* 2013).

$$\ln(q_e - q_t) = \ln q_e - k_1 t \tag{2}$$

$$\frac{t}{q_t} = \frac{1}{k_2 q_e^2} + \frac{t}{q_e} \tag{3}$$

where q_t (mg/g) is the adsorption capacity of absorbent in time 't', q_e (mg/g) is the saturated adsorption capacity of the absorbent at adsorption equilibrium, and k_1(min^{-1}), k_2 ($g{\cdot}mg^{-1}{\cdot}min^{-1}$) are the quasi-first and -second order rate constants of Lagergren, respectively. A plot of ln ($q_e - q_t$) and t/q_t versus t gave a linear relationship from which comes the value of k_1 and q_e, and k_2 and q_e. As indicated in Figure 6(a) and 6(b), the correlation coefficient (R^2) of COD (0.9647) and PFCs (0.9110) for the second order kinetic model was greater than that of the first order kinetic model (0.8856 and 0.8569), which indicated that the

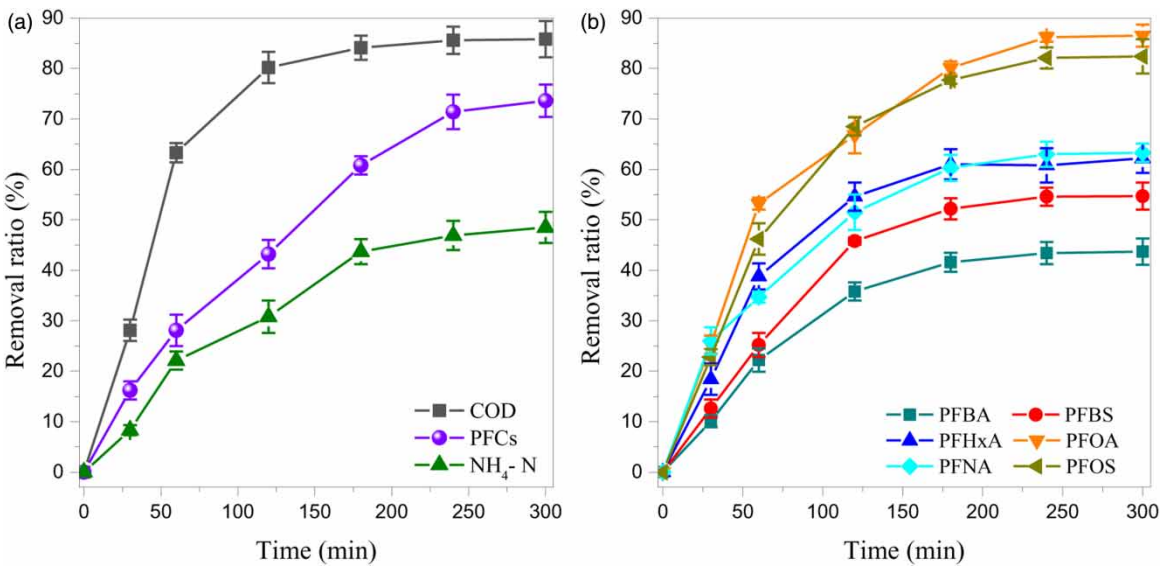

Figure 5 | Competitive adsorption of COD, NH_4-N and PFCs.

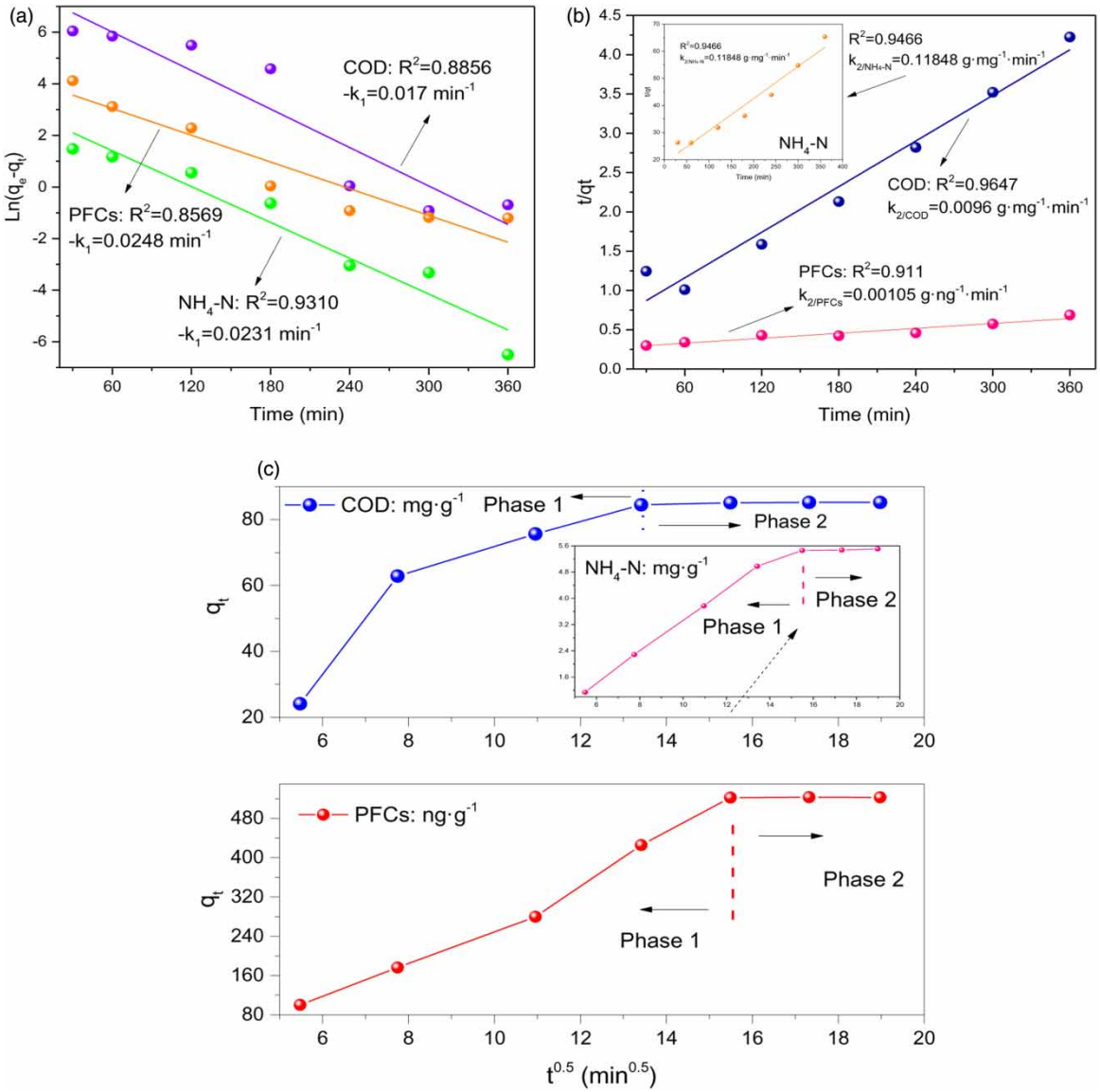

Figure 6 | Fitting curves of Lagergren quasi-first (a), second order dynamic equation (b), and intraparticle diffusion model of COD, NH_4-N and PFCs (c).

adsorption process involved the process of liquid film diffusion, intraparticle diffusion, and chemical reaction that lines with this research. This is reasonable, because the ZnO/AC could not only adsorb the contaminants through adsorption, but also degrade them through ZnO photocatalytic reaction. To deeply investigate the diffusion rate and steps in the adsorbent, the assumptions of the internal diffusion model was to ignore the diffusion resistance of the liquid film, and that the diffusion mode was random. According to the internal diffusion model formula (Equation (4)), a plot between 'q_t' versus 't' gave a linear relationship from which k_{ip} (internal diffusion rate constant) could be determined.

$$q_t = k_{ip} t^{0.5} + C \quad (4)$$

As presented in Figure 6(c), the fitted model of COD and PFCs could be split into two linear relationships (phase 1 and 2), suggesting that the adsorption process was affected by the intraparticle diffusion and the liquid film diffusion. Meanwhile, the adsorption process of COD showed a good linear relationship in the first two hours, indicating that the organic matter was adsorbed on the surface of ZnO/AC after passing through the

liquid film in this period. Furthermore, most of the pollutants simultaneously underwent a diffusion process within the particles while the pollutants were accumulated to a certain extent that led to the adsorption rate being controlled by both processes.

Mechanism investigation

Previous studies have demonstrated that the adsorption of pollutants in aqueous solutions by activated carbon depends on numerous factors such as porosity, microstructure, and the physical-chemical properties of activated carbon (Maneerung *et al.* 2016). Because the high bond energy of C-F in PFCs and the low Van der Waals force of the fluorine atom caused a strong polarity of C-F bond, the reaction between negatively charged nucleophiles and carbon atoms could be blocked. However, the doping of ZnO could change the ratio of micropores and mesopores, and provided more positive charge to increase the reactive sites on the activated carbon surface (Ochoa-Herrera & Sierra-Alvarez 2008). Additionally, due to the photoelectric property of ZnO, it is believed that photodegradation processes were involved in the removal of COD and PFCs. As depicted in Figure 7, when ZnO/AC was irradiated with solar light, charge separation produced an electron-hole pair (h^+_{vb}/e^-_{cb}). During the photosensitization process, the AC was excited to a higher energy state and transferred its electron to the conduction band of ZnO. The conduction band electrons were then transferred to the ZnO/AC surface before the conduction band electrons generated •OH radicals by reacting with O_2 (Raizada *et al.* 2014). The valence band holes reacted with H^+/H_2O at the adsorption catalyst surface to produce •OH equally (He *et al.* 2018). As a result, the •OH in the solution could oxidize and degrade some organic matter that contributed to the elimination of toxic pollutants.

Regeneration of saturated ZnO/AC

The ultrasonic method was used for the regeneration of ZnO/AC owing to its convenience and the high efficiency at which the mechanical and cavitation effect of an ultrasonic wave can effectively promote the regeneration of activated carbon (Yu *et al.* 2014). In this work, the saturated ZnO/AC was regenerated by ultrasonic method and the removal efficiency of PFCs was used to evaluate the adsorption performance of ZnO/AC after regeneration. Multiple experimental results indicated the PFCs removal efficiencies could reach 55.8, 63.4, 68.5, and 64.9% after 1, 2, 3, and 4 h of ultrasonic durations, which suggesting that 3 h of ultrasonic duration could effectively remove the adsorbed pollutants in the ZnO/AC pores and achieved a regeneration state. The SEM images (Figure 8) reveal that the morphological and microstructure characteristics of ZnO/

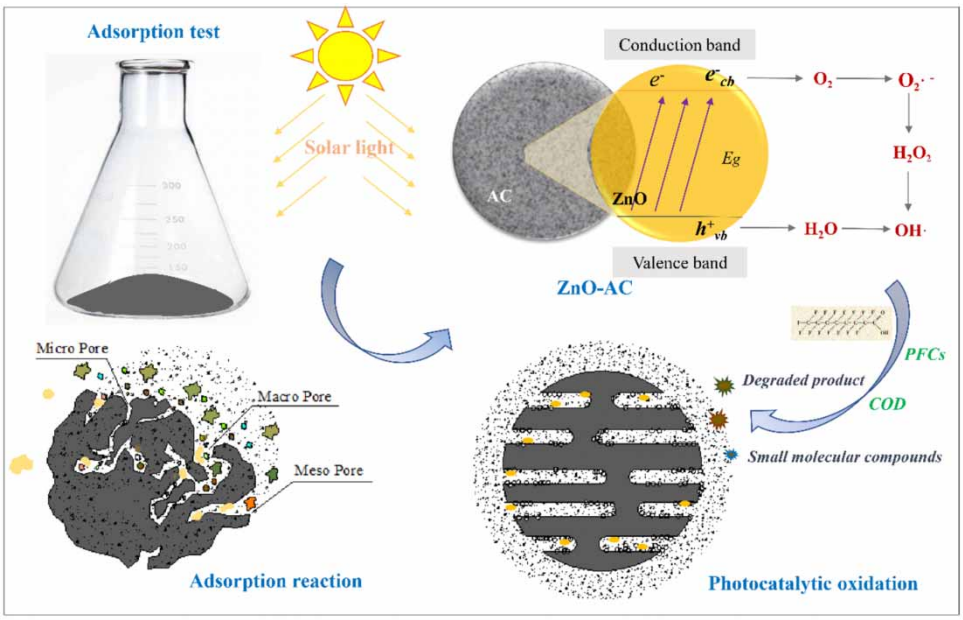

Figure 7 | Schematic diagram of adsorption mechanism.

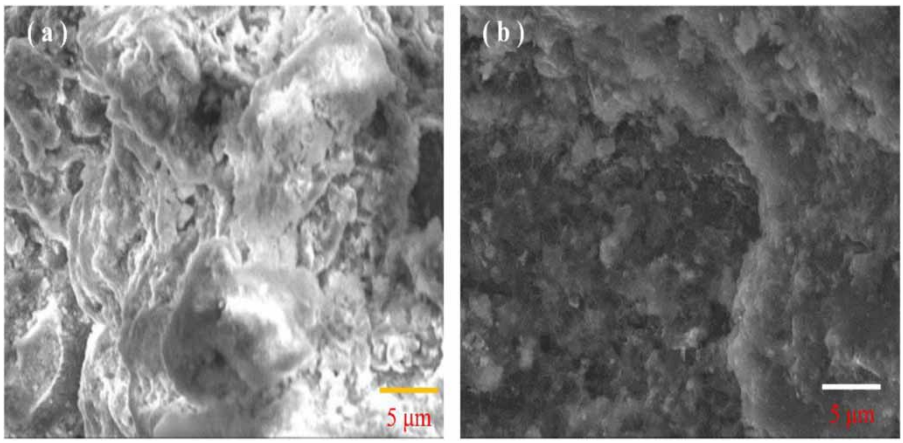

Figure 8 | SEM images of saturated ZnO/AC (a) and ultrasonic regenerated ZnO/AC (b).

AC after used was wrapped up by pollutants, while obvious pores could be seen on the surface after regeneration, which exhibited good regeneration ability.

CONCLUSIONS

In this study, ZnO/AC was prepared using the homogeneous precipitation method and was used to remove contaminants in a wastewater treatment plant effluent. The results indicated that the ZnO/AC absorbent had a significant effect on the removal of pollutants under sunlight. The maximum removal efficiencies of the COD, PFOA, and PFOS reached 86.6%, 86.8%, and 82.1%, while the removal efficiencies of NH_4-N, PFBA, and PFBS were less than 56% at the optimal parameters of absorbent dosage 0.8 g/L and contact time of 240 min. Moreover, there was a competitive adsorption process between COD and PFCs in the following order: COD > PFOA > PFOS > PFNA > PFBS > PFBA. The study of the adsorption kinetics illustrated that the removal of contaminants in the effluent by ZnO/AC followed a Lagergren quasi-second order model. The effective elimination of PFCs in this study was conducive to facilitating the further implication of toxicity reduction and indicated the significant potential of ZnO/AC absorbent in practical wastewater treatment.

ACKNOWLEDGEMENT

This work was supported by the National Key R & D Program of China (No. 2018YFC0406400).

DATA AVAILABILITY STATEMENT

All relevant data are included in the paper or its Supplementary Information.

REFERENCES

Ansari, F., Ghaedi, M., Taghdiri, M. & Asfaram, A. 2016 Application of ZnO nanorods loaded on activated carbon for ultrasonic assisted dyes removal: experimental design and derivative spectrophotometry method. *Ulrasonics Sonochemistry* **33**, 197–209.

Arvaniti, O. S., Ventouri, E. I., Stasinakis, A. S. & Thomaidis, N. S. 2012 Occurrence of different classes of perfluorinated compounds in Greek wastewater treatment plants and determination of their solid–water distribution coefficients. *Journal of Hazardous Materials* **239**, 24–31.

Aydin, H., Bulut, Y. & Yerlikaya, C. 2008 Removal of copper (ii) from aqueous solution by adsorption onto low-cost adsorbents. *Journal of Environmental Management* **87** (1), 37–45.

Fagbayigbo, B. O., Opeolu, B. O., Fatoki, O. S. & Olatunji, O. S. 2018 Validation and determination of nine PFCs in surface water and sediment samples using UPLC-QTOF-MS. *Environmental Monitoring and Assessment* **190** (6), 346–351.

Fromme, H., Mosch, C., Morovitz, M., Alba-Alejandre, I., Boehmer, S. & Kiranoglu, M. 2010 Pre-and postnatal exposure to perfluorinated compounds (PFCs). *Environmental Science & Technology* **44** (18), 7123–7129.

He, X., Ding, L., Su, W., Ma, H., Huang, H. & Wang, Y. 2018 Distribution of endotoxins in full scale pharmaceutical wastewater treatment plants and its relationship with microbial community structure. *Water Science & Technology* **77** (10), 2397.

Hori, H., Nagaoka, Y., Yamamoto, A., Sano, T., Yamashita, N. & Taniyasu, S. 2006 Efficient decomposition of environmentally persistent perfluorooctanesulfonate and related

fluorochemicals using zerovalent iron in subcritical water. *Environmental Science & Technology* **40** (3), 1049–1054.

Jian, J. M., Guo, Y., Zeng, L., Liangying, L., Lu, X. & Wang, F. 2017 Global distribution of perfluorochemicals (PFCs) in potential human exposure source – a review. *Environment International* **108**, 51–62.

Lu, Q. & Zhou, J. W. 2012 Simulated calculation of hourly solar radiation intensity and optimum inclination angle of solar collector in clear days in major cities of China. *Building Science* **28** (S2), 22–26 (in Chinese).

Maneerung, T., Liew, J., Dai, Y., Kawi, S., Chong, C. & Wang, C. H. 2016 Activated carbon derived from carbon residue from biomass gasification and its application for dye adsorption: kinetics, isotherms and thermodynamic studies. *Bioresource Technology* **200**, 350–359.

Moriwaki, H., Takagi, Y., Tanaka, M., Tsuruho, K., Okitsu, K. & Maeda, Y. 2005 Sonochemical decomposition of perfluorooctane sulfonate and perfluorooctanoic acid. *Environmental Science & Technology* **39** (9), 3388–3392.

Niu, J., Lin, H., Gong, C. & Sun, X. 2013 Theoretical and experimental insights into the electrochemical mineralization mechanism of perfluorooctanoic acid. *Environmental Science & Technology* **47** (24), 14341–14349.

Niu, Z., Wang, Y., Hui, L., Jin, F., Yang, L. & Niu, J. 2017 Electrochemically enhanced removal of perfluorinated compounds (PFCs) from aqueous solution by CNTs-graphene composite electrode. *Chemical Engineering Journal* **328** (15), 228–235.

Ochoa-Herrera, V. & Sierra-Alvarez, R. 2008 Removal of perfluorinated surfactants by sorption onto granular activated carbon, zeolite and sludge. *Chemosphere* **72** (10), 1588–1593.

Raizada, P., Singh, P., Kumar, A., Sharma, G., Pare, B. & Jonnalagadda, S. B. 2014 Solar photocatalytic activity of nano-ZnO supported on activated carbon or brick grain particles: role of adsorption in dye degradation. *Applied Catalysis A-General* **486**, 159–169.

Senevirathna, S. T., Tanaka, S., Fujii, S., Kunacheva, C., Harada, H. & Shivakoti, B. R. 2010 A comparative study of adsorption of perfluorooctane sulfonate (PFOS) onto granular activated carbon, ion-exchange polymers and non-ion-exchange polymers. *Chemosphere* **80** (6), 647–651.

Seo, S. H., Son, M. H., Choi, S. D. & Chang, Y. S. 2018 Influence of exposure to perfluoroalkyl substances (PFASs) on the Korean general population: 10-year trend and health effects. *Environment International* **113**, 149–161.

Shi, Y., Pan, Y., Yang, R., Wang, Y. & Cai, Y. 2010 Occurrence of perfluorinated compounds in fish from Qinghai-Tibetan Plateau. *Environment International* **36** (1), 46–50.

Shibin, O. M., Yesodharan, S. & Yesodharan, E. P. 2015 Sunlight induced photocatalytic degradation of herbicide diquat in water in presence of ZnO. *Journal of Environmental Chemical Engineering* **3** (2), 1107–1116.

Sorlini, S., Biasibetti, M., Collivignarelli, M. C. & Crotti, B. M. 2015 Reducing the chlorine dioxide demand in final disinfection of drinking water treatment plants using activated carbon. *Environmental Technology* **36**, 1499–1509.

Su, P. D., Li, Y., Zhang, J. K. & Li, Y. D. 2019 Characterization and chemical fixation of stainless steel pickling residue using sodium sulfide hydrate. *Environmental Science and Pollution Research* **26**, 10240–10250.

Tomy, G. T., Pleskach, K. & Ferguson, S. H. 2009 Trophodynamics of some PFCs and BFRs in a Western Canadian Arctic Marine Food Web. *Environmental Science & Technology* **43** (11), 4076–4081.

Wang, Y., Zhong, Y., Li, J., Zhang, J., Lyu, B., Zhao, Y. & Wu, Y. 2018 Occurrence of perfluoroalkyl substances in matched human serum, urine, hair and nail. *Journal of Environmental Sciences* **67** (5), 194–200.

Xi, D. L., Sun, Y. S. & Liu, X. Y. 2008 *Environmental Monitoring*. Higher Education Press, Beijing, China.

Yong, H., Shen, Z., Ye, W., Wang, X., Zhang, S. & Shi, X. 2016 Amorphous ZnO based resistive random access memory. *RSC Advances* **6** (22), 17867–17872.

Yu, J., He, C., Liu, X., Wu, J., Hu, Y. & Zhang, Y. 2014 Removal of perfluorinated compounds by membrane bioreactor with powdered activated carbon (PAC): adsorption onto sludge and PAC. *Desalination* **334** (1), 23–28.

Zhang, C., Jiang, S., Tang, J., Zhang, Y., Cui, Y. & Su, C. 2018 Adsorptive performance of coal based magnetic activated carbon for perfluorinated compounds from treated landfill leachate effluents. *Process Safety and Environmental Protection* **117**, 383–389.

Zhou, M., Gao, X., Yong, H., Chen, J. & Xiao, H. 2013 Uniform hamburger-like mesoporous carbon-incorporated ZnO nanoarchitectures: one-pot solvothermal synthesis, high adsorption and visible-light photocatalytic decolorization of dyes. *Applied Catalysis B: Environmental* **138** (21), 1–8.

First received 25 January 2020; accepted in revised form 18 June 2020. Available online 30 June 2020